UDK 004.85 : 539.1.074 + 519.65

Machine learning augmented Tikhonov regularization with iterative approach for stable neutron spectrum unfolding

Chizhov K.A. (Joint Institute for Nuclear Research, Dubna State University)

Shirkov S.G. (Joint Institute for Nuclear Research)

Chizhov A.V. (Joint Institute for Nuclear Research)

A hybrid multi-stage algorithm is developed for solving the ill-posed inverse problem of unfolding the neutron energy spectrum from multi-sphere Bonner spectrometer measurements. Traditional approaches, such as Tikhonov regularization and iterative methods, have significant limitations due to the subjective choice of the regularization parameter or initial approximation, which compromises the solution's stability and accuracy. In the proposed method, the first stage automated machine learning (autoML) is used to find the optimal model to predict the global spectral shape. The second stage applies Tikhonov regularization, where regularization parameter is objectively optimized based on a similarity metric relative to the autoML prediction. The smoothing functional is minimized using convex optimization techniques. The third stage utilizes the obtained solution as the initial guess for an iterative refinement procedure. Physical prior knowledge is incorporated both through a parametrically generated training dataset (weighted sums of fission, evaporation, Gaussian, and high-energy spectral components). The hybrid approach demonstrates superior robustness to noisy input data compared to methods using solely Tikhonov regularization or machine learning. The developed methodology is applicable to neutron dosimetry at high-energy nuclear facilities and for solving a broad class of inverse problems described by Fredholm integral equations of the first kind.

Keywords: neutron spectrum unfolding, Tikhonov regularization, machine learning, autoML, iterative methods, Bonner sphere spectrometer, inverse problems.

1. Introduction

1.1. Problem Relevance

Accurate characterization of a wide range neutron energy spectra from eV to hundreds of MeV is necessary for radiation protection, shielding design and dosimetry for personnel of particle accelerators. Neutrons (as uncharged particles) require indirect detection methods. The Bonner Sphere Spectrometer (BSS) as a thermal neutron detector surrounded by polyethylene

moderators of varying diameters, is the most widely used instrument for neutron spectrometry [1]. However, calculating the neutron energy spectrum $\varphi(E)$ from the set of BSS readings constitutes an ill-posed inverse problem, described by a system of Fredholm integral equation of the first kind. This ill-posedness, characterized by non-uniqueness and high sensitivity to measurement noise, necessitates specialized unfolding techniques.

1.2. Problem Statement

The relationship between the neutron spectrum ϕ and the BSS readings for M spheres is given by:

$$Q_j = \int_{E_{\min}}^{E_{\max}} R_j(E)\,\phi(E)\,dE, \quad j = 1, \ldots, M, \tag{1}$$

where $R_j(E)$ is the response function of the j-th sphere [2]. Q_j is the Bonner spectrometer reading including measurement error ϵ, E – energy.

Since the unfolding of the neutron spectrum is assumed to be a fairly wide energy range that exceeds 11 orders of magnitude, to reduce the error of numerical integration it is convenient to convert it to a new variable called lethargy $u(E) = \lg(E/E_{\min})$:

$$\ln 10 \times \int_0^{l_E} K_j(u)\,\phi(u)\,E(u)\,du = Q_j, \quad j = 1, \ldots, M, \tag{2}$$

where $l_E = \lg(E_{\max}/E_{\min})$.

The integrand form suggests finding $\varphi(u) = \phi(u) \cdot E(u)$, which we continue to call the neutron spectrum.

Discretizing the energy into N bins ($N \gg M$) transforms (2) into a system of linear equations:

$$\mathbf{A}\boldsymbol{\varphi} = \mathbf{q}, \tag{3}$$

where $\mathbf{A} \in \mathbb{R}^{M\times N}$ is the response matrix, $\boldsymbol{\varphi} \in \mathbb{R}^N$ is the discretized fluence spectrum, and $\mathbf{q} \in \mathbb{R}^M$ is the vector of measured counts. The system is underdetermined and ill-conditioned.

This inverse problem can be reformulated as a machine learning regression task. The input features are the M normalized BSS readings $\tilde{q}_j = q_j/k_j$, where $k_j = \sum_{i=1}^{M} q_i$. The target output is the discretized spectrum vector $\boldsymbol{\varphi}$. The ML model $\mathcal{F}$ learns the mapping:

$$\tilde{\boldsymbol{\varphi}}_{\text{pred}} = \boldsymbol{k}\mathcal{F}(\tilde{\mathbf{q}}). \tag{4}$$

1.3. Existing Approaches and Related Work

Neutron spectra unfolding methods include iterative algorithms (e.g., MLEM [3], Landweber [4]), maximum entropy deconvolution (MAXED) [5], Tikhonov regularization [6], TSVD [4], stochastic methods like genetic algorithms [8], parametric [9, 10] and other methods [11]. However, the results of application of a method depends on the chosen parameters. For iterative methods, the initial approximation and the choice of the number of iterations are important. For regularization methods, the choice of the regularization parameter can over smooth the solution or create nonphysical ripples in the spectrum if the parameter is too small. In unfolding process it is necessary to consider the physical correctness of the spectrum: smoothness and non-negativity. Conditional stability of the solution is needed, other war small errors in BSS readings may produce large uncertainty in spectra.

Machine learning [13] and neural networks (NN) [7, 14] of different types and architecture has been increasingly applied to this problem, including deep learning frameworks with input feature transformations [15], Kolmogorov-Arnold networks [16], radial basis function [17], convolutional [18], generalized regression [19] and Bayesian NN [20]. For interpretation of the neural network spectrum prediction, explainable artificial intelligence (XAI) methods such as SHAP [13], LIME [21], ANFIS-based [22] were applied.

ML models are typically trained on synthetic datasets generated via Monte Carlo codes [18] or parametric models [23]. A set of real spectra may also be incorporated into the dataset [13] with assumption that these spectra have been accurately unfolded via the methods employed by the authors. These datasets pair a neutron spectra with their corresponding BSS responses.

Finding the optimal model requires iterating over both the algorithms themselves and the model's hyperparameters, as well as consuming a significant amount of computational time. automatic ML AutoML frameworks [24], which include algorithms for efficiently finding hyperparameters within a given time, help with this.

However, data-driven ML approaches can struggle with generalization to spectra outside the training distribution and may lack physical consistency, for example producing negative fluence values or being overly sensitive to input noise. Therefore, the authors proposed in this work a synergistic approach: an ML model provides a rapid, data-driven initial guess, which is then refined and regularized by well-established iterative physical models, combining the speed of ML with the stability and physical grounding of traditional methods, as it was made in [25] for the dataset of 201 neutron energy spectra and the corresponding measured responses from [2] .

In this paper we propose a method with combination of algorithms, where on the first

stage autoML trained on a large synthetic dataset is used to find the optimal model to predict the global spectral shape. This shape was the init spectra for next method. For Tikhonov regularization unfolding, regularization parameter is objectively optimized based on a similarity metric relative to the autoML prediction. The smoothing functional is minimized using convex optimization techniques. For iterative methods, the unfolded by other method spectra was the initial guess. The uncertainty in spectrum unfolding was estimated using a Monte Carlo simulation for a set of random samples and a normally distributed error. Combining the methods yielded a robust solution for the error in the initial data.

2. Materials and Methods

2.1. Synthetic Dataset Generation

A dataset of 5×10^5 neutron spectra was generated. Each spectrum $\varphi(E)$ is modeled as a linear combination of four parametric functions [26]:

$$\varphi(E) = P_{\text{th}}\varphi_{\text{th}}(E) + P_{\text{e}}\varphi_{\text{e}}(E) + P_{\text{f}}\varphi_{\text{f}}(E) + P_{\text{hi}}\varphi_{\text{hi}}(E), \tag{5}$$

representing thermal, epithermal, fast, and high-energy components, respectively, with weights summing to unity. The energy range was 10^{-9} MeV to 6.31 MeV, discretized into $N = 60$ logarithmic bins.

For each spectrum, the readings $\mathbf{q}$ for a 10 sphere BSS GSF [2] (with diameters: 0, 2, 3, 5, 6, 8, 10, 12, 15, 18 inches) were calculated by convolving the spectrum with response functions $\mathbf{A}$. The dataset was split into training (70%) and testing (30%) sets.

2.2. Machine Learning Model and Feature Processing

In this work we used H2O – an ML framework for algorithm selection, feature generation, hyperparameter tuning, iterative modeling and model assessment. The H2O AutoML uses a combination of fast random search and stacked ensembles to achieve the best model metrics. H2O AutoML includes XGBoost Gradient Boosting Machines (GBM), Random Forests, Deep Neural Networks and Generalized Linear Models (GLM).

We trained $N = 60$ independent models for each energy bin. Each was trained to predict the normalized spectrum $\tilde{\boldsymbol{\varphi}}$ from the normalized BSS readings $\tilde{\mathbf{q}}$. Model performance was evaluated using the coefficient of determination R^2 and $RMSE$. A post-processing step sets all negative

values in $\boldsymbol{\varphi}_{\mathrm{ML}}$ to zero to ensure physical correctness before it is used as an initial guess for iterative methods.

2.3. Refinement Algorithms

2.3.1. Tikhonov Regularization

The solution is found by minimizing the regularized functional (6):

$$\boldsymbol{\varphi}^* = \arg\min_{\boldsymbol{\varphi}\geq 0} \left\{ \|\mathbf{A}\boldsymbol{\varphi} - \mathbf{q}\|_2^2 + \lambda^2 \|\mathbf{L}\boldsymbol{\varphi}\|_2^2 \right\}, \tag{6}$$

where $\mathbf{L}$ is the identity matrix (zeroth-order Tikhonov) and $\lambda \geq 0$ is the regularization parameter. The parameter λ is chosen to maximize the similarity metric between the Tikhonov solution and the ML estimate $\boldsymbol{\varphi}_{\mathrm{ML}}$. In this work a cosine similarity [27] was chosen as the metric (7). It is a measure of similarity between two non-zero vectors in n-dimensional space. For spectra the values of the vector cannot be negative, so for our task the value of cosine similarity is bounded in [0,1]. Two proportional vectors (spectra) have a cosine similarity of 1, two orthogonal vectors have a similarity of 0.

The algorithm was developed as a python code with *CVXPY* [28] package and ECOS [29] convex solver.

$$\lambda^* = \arg\max_{\lambda} \frac{\langle \boldsymbol{\varphi}(\lambda), \boldsymbol{\varphi}_{\mathrm{ML}} \rangle}{\|\boldsymbol{\varphi}(\lambda)\| \|\boldsymbol{\varphi}_{\mathrm{ML}}\|}. \tag{7}$$

2.3.2. Maximum Likelihood Expectation Maximization

Maximum Likelihood Expectation Maximization is an iterative process that maximizes the likelihood of obtaining the measured data when convergence is achieved, providing an accurate neutron spectrum [30]. The MLEM algorithm iteratively updates the spectrum estimate for k steps:

$$\varphi_i^{(k+1)} = \frac{\varphi_i^{(k)}}{\sum_{j=1}^{M} A_{ji}} \sum_{j=1}^{M} \frac{q_j A_{ji}}{\sum_{l=1}^{N} A_{jl} \varphi_l^{(k)}}, \quad i = 1, \ldots, N, \tag{8}$$

starting from the ML estimate $\boldsymbol{\varphi}^{(0)} = \boldsymbol{\varphi}_{\mathrm{ML}}$.

The algorithm was developed as a python code with *ODL* [3] package.

2.3.3. Landweber Iteration

The Landweber iteration is a gradient descent method for solving $\mathbf{A}\boldsymbol{\varphi} = \mathbf{q}$:

$$\boldsymbol{\varphi}^{(k+1)} = \boldsymbol{\varphi}^{(k)} + \alpha \mathbf{A}^T (\mathbf{q} - \mathbf{A}\boldsymbol{\varphi}^{(k)}), \tag{9}$$

with relaxation parameter α chosen as $\alpha = 1/\|\mathbf{A}^T\mathbf{A}\|_2$, and initialized with $\boldsymbol{\varphi}^{(0)} = \boldsymbol{\varphi}_{\mathrm{ML}}$, for chosen k steps.

These unfolding methods were implemented to the python package *bssunfold* [31].

2.4. Robustness Evaluation

To assess stability against measurement uncertainties, random Gaussian noise with a relative standard deviation of $\zeta_Q = 1\%$ was added to the simulated detector readings $\mathbf{q}$. For $N_{random} =$ 500 random samples of readings spectra were unfolded by methods and by mixture of methods.

2.5. Effective dose rate assessment

In accordance with radiation safety standards [32], personnel exposure to neutrons should be below certain levels. Therefore, the effective dose rate for the isotropic irradiation was used as one of metrics for comparison of the quality of unfolding, eq. (10).

$$\dot{H} = \int_{E_{min}}^{E_{max}} \phi(E) \cdot h(E) dE, \tag{10}$$

where $\dot{H}$ is the effective dose rate, $h(E)$ is the corresponding dose conversion coefficient [33], for monoenergetic particles in a certain irradiation geometry (ISO) [2]. For each unfolded spectrum the $\dot{H}$ was calculated.

2.6. Spectra similarity metrics

To assess the quality of spectrum unfolding, we used metrics such as MAE, MSE, Wasserstein distance, cosine similarity and the effective dose rate [24]. This set of metrics allows us to evaluate the unfolding quality for both individual energy bins and the spectrum shape as a whole.

3. Results

3.1. ML Model Performance

Models were trained on the HybriLIT platform. It achieved an accuracy comparable to the values we had previously obtained using other ML algorithms [13, 15], mean R^2 on training set is 0.92 and mean R^2 on test set – 0.86. H2O autoML framework found XGBoost and GBM as the best models with individual hyperparameters for each model.

3.2. Results for ^{252}Cf spectra

The ML models were validated using reference spectra ^{252}Cf for GSF BSS [2]. This spectrum is good for validation; it can be measured experimentally using other methods or calculated using Monte Carlo programs. It has one peak, and the rest of the neutron energy range is zero. Accordingly, if the unfolding method produces oscillations near zero or negative values, this will be visible on the spectrum. The ML model reconstructed the spectrum quite well, correctly identifying the peak, although slightly undershooting it. There are some minor artifacts on the right side of the spectrum. Effective BSS readings were calculated by eq. (3) and are close to real measurements, Fig. 1.

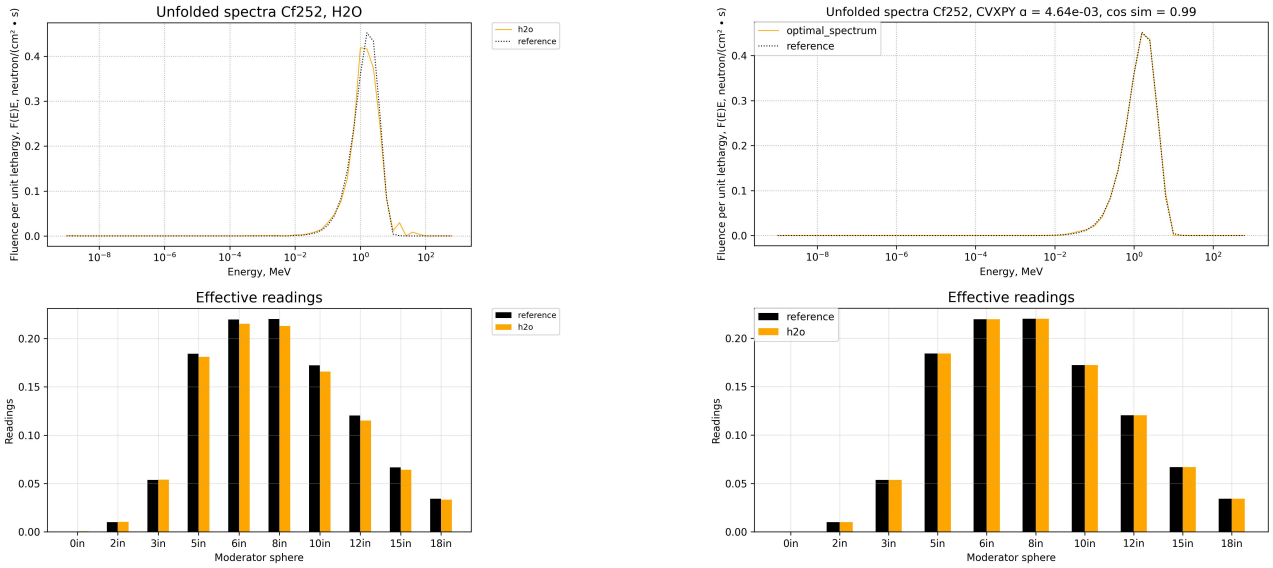

(a) (b)

Figure 1. (a) – reference and unfolded by H2O autoML spectra for ^{252}Cf and effective BSS readings, (b) – Tikhonov regularization with parameter selected according to the best cosine similarity with H2O spectrum.

MLEM and Lanweber iterative algorithms with an uniform spectrum as the initial approximation yield better results than the ML, with slightly lower peak heights. With the correct selection of the regularization parameter, Tikhonov's method gives the best result, a near-perfect match, Fig. 2. But if we use use a combination of methods, then the initial approximation from ML allows both the iterative and regularization methods to obtain excellent agreement with reference spectra, Fig. 1,2.

3.3. Results for GRENF, position C spectra

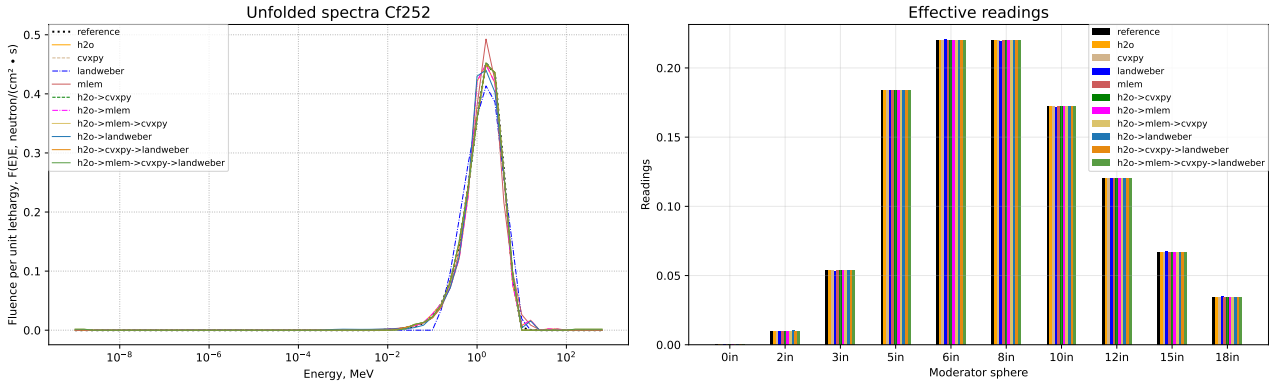

Figure 2. Comparison of reference and unfolded spectra and readings for ^{252}Cf.

The ML models was validated also on the Monte-Carlo calculated spectra from GSF realistic neutron field facility (GRENF), for position C that corresponds to a specific physical placement of the dosimeter relative to the plutonium source with significant scattering from surrounding materials [2]. This spectra has a wide neutron energy and it has a sharp peak, that is difficult to unfold.

Although the algorithms selected spectra with almost ideal values of effective readings, the shape of the spectra themselves is different, Fig. 3.

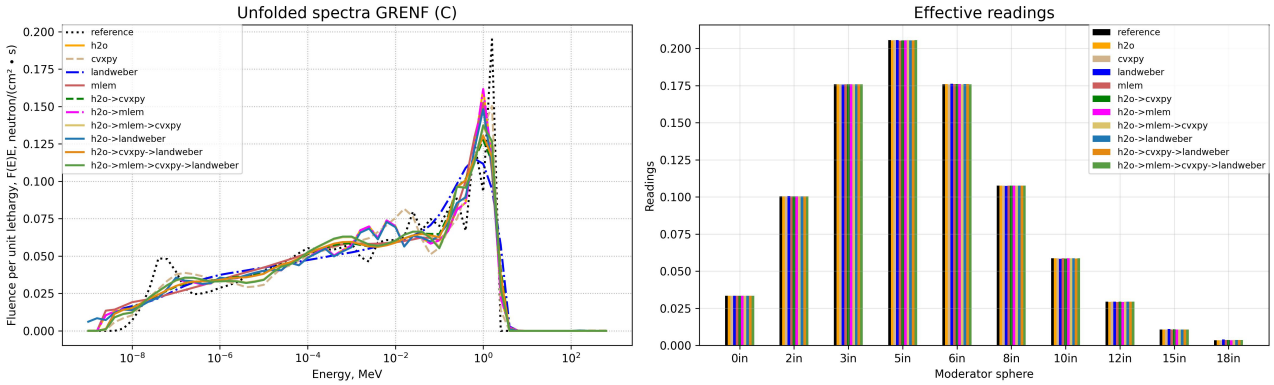

Figure 3. Reference and unfolded by separate and combinations of algorithms spectra for GRENF, position C.

For precise measurements, the CVXPY method shows the best result, table 1. However, the spectrum unfolding results for other methods we used are also quite good, with $\Delta\dot{H} < 1\%$. Additional information from H20 improves the spectrum unfolding quality of the iterative algorithms.

3.4. Stability Analysis

Table 1

GRENF(C). Metrics for assessing the similarity of a spectrum to a reference one for various unfolding methods.

method	R^2	CS	MSE
H2O	0.79	0.95	2.7×10^{-4}
cvxpy	0.89	0.97	1.4×10^{-4}
landweber	0.76	0.94	3.1×10^{-4}
mlem	0.79	0.95	2.8×10^{-4}
H2O-cvxpy	0.83	0.96	2.2×10^{-4}
H2O-mlem	0.79	0.95	2.7×10^{-4}
H2O-mlem-cvxpy	0.86	0.97	1.9×10^{-4}
H2O-landweber	0.80	0.95	2.6×10^{-4}
H2O-cvxpy-landweber	0.84	0.96	2.1×10^{-4}
H2O-mlem-cvxpy-landweber	0.86	0.97	1.9×10^{-4}
H2O-cvxpy-mlem	0.83	0.96	2.2×10^{-4}

method	WD	$\Delta\dot{H}, \%$	$\Delta\mathbf{q}$
H2O	3.8×10^{-1}	0.7%	3.0×10^{-4}
cvxpy	3.6×10^{-1}	0.4%	8.2×10^{-13}
landweber	3.8×10^{-1}	0.2%	7.6×10^{-4}
mlem	4.5×10^{-1}	0.8%	4.8×10^{-4}
H2O-cvxpy	3.1×10^{-1}	0.6%	3.1×10^{-4}
H2O-mlem	3.8×10^{-1}	0.7%	3.0×10^{-4}
H2O-mlem-cvxpy	2.8×10^{-1}	0.3%	1.6×10^{-4}
H2O-landweber	4.3×10^{-1}	0.5%	2.8×10^{-4}
H2O-cvxpy-landweber	2.8×10^{-1}	0.3%	3.0×10^{-4}
H2O-mlem-cvxpy-landweber	2.9×10^{-1}	0.4%	1.4×10^{-4}
H2O-cvxpy-mlem	3.1×10^{-1}	0.6%	3.1×10^{-4}

Measurement results always contain errors. In ill-posed problems, small errors in the input data can lead to large errors in the solution. Therefore, we proposed combination of methods to stabilize the solution. Spectra were unfolded for input noise level ζ_Q and N_{random} samples. For evaluation metrics from 2.6 we obtained results presented in table 2.

Table 2

GRENF(C). Average metrics with standard deviation for assessing the similarity of a spectrum to a reference one for various

method	R^2	CS	MSE
H2O	0.69 ± 0.09	0.93 ± 0.02	$(4 \pm 1.2) \times 10^{-4}$
cvxpy	-5.03 ± 4.15	0.55 ± 0.16	$(7.9 \pm 5.4) \times 10^{-3}$
landweber	0.75 ± 0.02	0.94 ± 0.01	$(3.3 \pm 0.3) \times 10^{-4}$
mlem	0.76 ± 0.03	0.94 ± 0.01	$(3.1 \pm 0.4) \times 10^{-4}$
H2O-cvxpy	0.76 ± 0.04	0.94 ± 0.01	$(3.1 \pm 0.5) \times 10^{-4}$
H2O-mlem	0.69 ± 0.09	0.93 ± 0.02	$(4 \pm 1.2) \times 10^{-4}$
H2O-mlem-cvxpy	0.73 ± 0.08	0.94 ± 0.02	$(3.5 \pm 1.1) \times 10^{-4}$
H2O-landweber	0.69 ± 0.09	0.93 ± 0.02	$(4 \pm 1.2) \times 10^{-4}$
H2O-cvxpy-landweber	0.73 ± 0.09	0.94 ± 0.02	$(3.5 \pm 1.2) \times 10^{-4}$
H2O-mlem-cvxpy-landweber	0.69 ± 0.13	0.93 ± 0.03	$(4 \pm 1.7) \times 10^{-4}$
method	WD	$\Delta\dot{H}, \%$	$\Delta\mathbf{q}$
H2O	0.63 ± 0.2	1.16	2.7×10^{-3}
cvxpy	2.33 ± 0.75	3.8	3.4×10^{-3}
landweber	0.48 ± 0.15	1.2	2.8×10^{-3}
mlem	0.52 ± 0.12	0.97	2.6×10^{-3}
H2O-cvxpy	0.52 ± 0.16	1.18	2.8×10^{-3}
H2O-mlem	0.63 ± 0.2	1.16	2.7×10^{-3}
H2O-mlem-cvxpy	0.68 ± 0.24	1.41	2.9×10^{-3}
H2O-landweber	0.74 ± 0.25	1.49	2.9×10^{-3}
H2O-cvxpy-landweber	0.7 ± 0.27	1.53	2.9×10^{-3}
H2O-mlem-cvxpy-landweber	0.81 ± 0.32	1.63	3×10^{-3}

For the GRENF(C) spectrum Figure 4 shows that the spectrum shape changes with errors in the source data: the range of possible spectra is shown in the semi-transparent area. Iterative

algorithms, which converge to a spectrum similar to the true one despite the error, prove to be the most stable. Tikhonov's method with convex optimization (CVXPY) produces excellent results with accurate data, but small errors significantly alter the spectrum shape. To achieve conditional stability of the solution, we propose using iterative methods. This yields a more accurate solution and reduces the uncertainty range. A combination of methods allows for the highest accuracy with an acceptable error. Selecting a regularization parameter based on the spectrum shape of the reconstructed ML yields significantly better results than using Tikhonov's method alone; the best result is $R^2 = 0.76$ for both the MSE $= 3.1 \times 10^{-4}$ and the MLEM method.

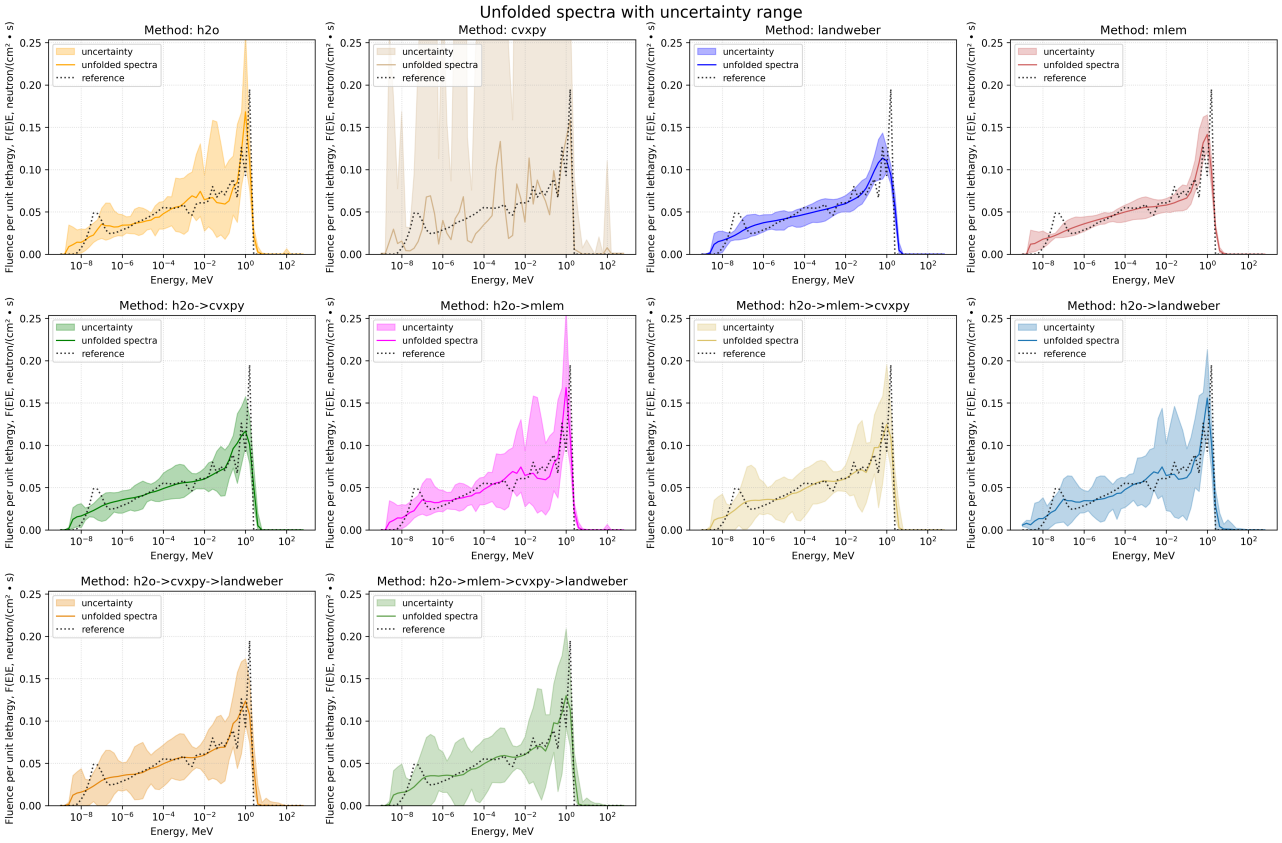

Figure 4. GRENF(C). Average unfolded spectra for developed unfolding algorithms, semi-transparent area shows the uncertainty of unfolding

4. Discussion

The results demonstrate that the proposed hybrid framework successfully leverages the complementary strengths of ML and analytical methods. The ML model provides a physically reasonable starting point that is already close to the true solution, effectively narrowing the solution space. This prior information is used in regularization and iterative algorithms and it

gives better results for MLEM and Landweber algorithms, if spectra has a complex form with sharp peaks.

The strategy of selecting the Tikhonov parameter λ by maximizing cosine similarity with the ML prior is a data-driven alternative to classical methods like the L-curve [34]. It automates parameter tuning and adapts it to the specific spectral shape suggested by the measurements, leading to more consistent performance. Of course, the result depends heavily on the trained model. It may fail to capture sharp peaks, which can be identified and unfolded more accurately with manual parameter selection (in accordance with the expert knowledge of spectra shape) and another solver such as Gurobi, Express [12, 28]. But if we don't know the shape, autoML selection can significantly improve the unfolding.

The primary limitation remains the dependence of the ML model on the quality and representativeness of the training data. Spectra very far from the FRUIT-generated distribution [9] may lead to poor initial guesses. The model metrics can be improved by incorporating a broader set of spectra from experimental and particle transport simulation software into the training dataset. Using combination of other types of ML algorithms and NN architectures with specific tabular data transformation [15, 35] can also yield better results.

Addition in the unfolding chain methods, such as variations of the conjugate gradient and quasi-Newton methods (e.g. L-BFGS-B [28, 36]) could also improve the unfolding results since they can give more accurate results than the methods used in this work [12].

The selection of the optimal set of moderator spheres is important for spectrum unfolding accuracy.It is necessary to ensure complete coverage of the neutron energy range. It is advisable to use spheres with the most diverse response functions. In practice, this means avoiding the use of multiple spheres of similar diameters. This reduces the correlation between the rows of the response matrix and lowers matrix's condition number [37, 38].

The most time is spent on training the model, since it needs to be trained for each set of moderator spheres and for each BSS. The method works quickly even for a trained model, allowing for the neutron spectra unfolding and assessment of doses to personnel. The method is implemented as a python code for cross-platform and convenient use by radiation safety specialists.

5. Conclusions

A hybrid multi-stage algorithm for neutron spectrum unfolding has been developed, combining a machine-learned prior with Tikhonov regularization and iterative algorithms (Landweber, MLEM). The algorithm uses an set of automatically fitted in H2O framework models (XGboost, GBM) trained on a large synthetic dataset to generate an initial spectrum estimate. This estimate is post-processed for physical consistency and then used to initialize the Tikhonov regularization process with the regularization parameter selected via optimization of cosine similarity.

The proposed approach was validated on a test set of spectra derived from Monte Carlo simulations: spectra for ^{252}Cf and realistic neutron field facility (GRENF). The stability against measurement noise compared to standalone ML or traditional unfolding algorithms was accessed.

It has been shown that the combination of a machine learning algorithm with a regularization method and the iteration algorithm provides high spectrum unfolding accuracy while reducing uncertainty caused by measurement errors. For example, with a measurement error of 1%, the error in estimation of the effective dose rate from the spectrum is 1.5%. In terms of the residual norm, the method yields effective reading values for BSS very close to the actual measurement data. The machine learning model has $R^2 = 0.69$, while the combined algorithm gives $R^2 = 0.76$.

This work establishes a practical and effective pipeline for spectra unfolding with machine learning and inverse problem solvers. The proposed method could be used for improving radiation protection in high-energy neutron fields.

5.0.1. Acknowledgments

Authors acknowledge the support of the JINR Multifunctional Information and Computing Complex for providing computational resources, http://hlit.jinr.ru.

5.0.2. Funding

This work was carried out within the framework of the state assignment of the Ministry of Education and Science of the Russian Federation (project No. 124112200072-2, "Application of Explainable Artificial Intelligence for the Interpretation of Machine Learning Algorithms").

References

1. Chizhov K., Beskrovnaya L., Chizhov A. Neutron spectrum unfolding method based on shifted legendre polynomials, its application to the IREN facility // Physics of Particles and Nuclei Letters. 2025. Vol. 22, no. 2. P. 190. DOI: https://doi.org/10.1134/S154747712470239X.
2. Compendium of Neutron Spectra and Detector Responses for Radiation Protection Purposes. Vienna: INTERNATIONAL ATOMIC ENERGY AGENCY, 2001. (Technical Reports Series; no. 403). ISBN 92-0-102201-8.
3. Adler J. et al. odlgroup/odl: ODL 0.7.0. Zenodo, 2018. DOI: 10.5281/zenodo.1442734.
4. Chizhov A., Chizhov K. TSVD-based neutron spectra unfolding by Bonner multi-sphere spectrometer readings with iteration procedure // The International Conference "Distributed Computing and Grid-technologies in Science and Education". 2025.
5. Borshchev D.S., Akimochkina M.A., Chizhov K.A. A hybrid method for neutron spectrum unfolding based on Tikhonov regularization and the MAXED algorithm. // 33rd International Conference "Mathematics. Computer. Education". 2026.
6. Chizhov K., Chizhov A. Optimization of the Neutron Spectrum Unfolding Algorithm Based on Tikhonov Regularization and Shifted Legendre Polynomials // MMCP 2024. 2024. P. 74.
7. Akimochkina M.A., Borshchev D.S., Chizhov K.A. Neural network reconstruction of neutron spectrum with a physically informed loss function // V Scientific and Practical Conference "Physical and Technical Intelligent Systems" (FTIS-2026): Book of abstracts. - Tambov: Yulis Publishing House LLC, 2026. P. 14. (in Russian).
8. Freeman D.W., Edwards D.R., Bolon A.E. Genetic algorithms–a new technique for solving the neutron spectrum unfolding problem // Nuclear Instruments and Methods in Physics Research Section A: Accelerators, Spectrometers, Detectors and Associated Equipment. 1999. Vol. 425, no. 3. P. 549–576.
9. Bedogni R., Domingo C., Esposito A., Fernández F. FRUIT: an operational tool for multisphere neutron spectrometry in workplaces // Nuclear Instruments and Methods in Physics Research Section A: Accelerators, Spectrometers, Detectors and Associated Equipment. 2007. Vol. 580, no. 3. P. 1301–1309.
10. Sannikov A.V., Peleshko V.N., Savitskaya E.N., et al. Multisphere neutron spectrometer based on the serial RSU-01 device // IHEP Preprint. 2007. Vol. 21.
11. Gómez-Ros J.M., Bedogni R., Domingo C., et al. Results of the EURADOS international comparison exercise on neutron spectra unfolding in Bonner spheres spectrometry // Radiation Measurements. 2022. Vol. 153. P. 106755.
12. Chizhov K.A., Chizhov A.V., Borshchev D.S., Akimochkina M.A. Methods for solving inverse problems for processing measurement results using the example of neutron spectrum unfolding // 33rd International Conference "Mathematics. Computer. Education". 2026.
13. Chizhov K. Random forest regression and Shapley additive explanation for effective dose rate estimation in high-energy neutron fields based on Bonner spectrometer measurements. Sirius, Sochi, 2025. URL: https://openreview.net/forum?id=S60GzItoqh (дата обращения : 21.05.2022).
14. Ortiz-Rodriguez J.M., Alfaro A.R., Haro A.R., et al. A neutron spectrum unfolding computer code

based on artificial neural networks // Radiation physics and chemistry. 2014. Vol. 95. P. 428–431.

15. Chizhov K., Bely A. Neutron spectrum unfolding using deep learning models for tabular data // Moscow University Physics Bulletin, 2025, Vol. 80, Suppl. 3, pp. S987–S995. DOI: 10.3103/S0027134925702832
16. Starikovskaya M.D., Chizhov K.A. Application of Kolmogorov-Arnold networks for solving the neutron spectrum unfolding problem // 33rd International Conference "Mathematics. Computer. Education". 2026.
17. Alvar A.A., Deevband M.R., Ashtiyani M. Neutron spectrum unfolding using radial basis function neural networks // Applied Radiation and Isotopes. 2017. Vol. 129. P. 35–41.
18. Bouhadida M., Mazzi A., Brovchenko M., et al. Neutron spectrum unfolding using two architectures of convolutional neural networks // Nuclear Engineering and Technology. 2023. Vol. 55, no. 6. P. 2276–2282.
19. Del Rosario Martinez-Blanco M., Ornelas-Vargas G., Castañeda-Miranda C.L., et al. A neutron spectrum unfolding code based on generalized regression artificial neural networks // Applied radiation and isotopes. 2016. Vol. 117. P. 8–14.
20. Zhou B., Hu Z., Zhong M., et al. Bayesian Neural Networks for the Neutron Spectrum Unfolding in the EAST Tokamak // IEEE Transactions on Instrumentation and Measurement. 2025.
21. Chizhov K. et al. Reconstruction of the energy spectrum of the neutron radiation flux using the random forest machine learning algorithm // Modern information technologies and IT education. 2024. Vol. 20, no. 4. (in Russian).
22. Chizhov K.A., Lebedev A.D., Trofimov Yu.V., et al. Interpretable neutron spectrum reconstruction based on two-stage ANFIS learning with SHAP regularization // 33rd International Conference "Mathematics. Computer. Education". 2026.
23. McGreivy J., Manfredi J.J., Siefman D. Data Augmentation for Neutron Spectrum Unfolding with Neural Networks // Journal of Nuclear Engineering. 2023. Vol. 4, no. 1. P. 77–95.
24. Chizhov K.A., Lebedev A.D., Trofimov Yu.V., et al. Automated machine learning spectrum unfolding for neutron spectrometry with Bonner spheres // The 11th International Conference "Distributed Computing and Grid-technologies in Science and Education July, 7-11, 2025 JINR, Dubna, Russia. 2025.
25. Shiwei L., Wenbao J., Wei C., et al. Neutron spectrum unfolding code based on iterative method combined with artificial neural networks for bonner sphere spectrometer // Journal of Radioanalytical and Nuclear Chemistry. 2024. Vol. 333, no. 1. P. 557–562.
26. Starikovskaya M.D., Chizhov K.A. Neutron spectrum unfolding based on random forest algorithm and generated training sample // Information and Telecommunication Technologies and Mathematical Modeling of High-Tech Systems 202. Russian University of Peoples' Friendship named after Patrice Lumumba, 2025. P. 389–394. (in Russian).
27. Condon Z.T. Unfolding Neutron Energy Spectra with a Passive Neutron Spectrometer: PhD thesis The Ohio State University, 2024.
28. Diamond S., Boyd S. CVXPY: A Python-embedded modeling language for convex optimization //

Journal of Machine Learning Research. 2016. Vol. 17, no. 83. P. 1–5.

29. Domahidi A., Chu E., Boyd S. ECOS: An SOCP solver for embedded systems // 2013 European control conference (ECC). IEEE, 2013. P. 3071–3076.
30. Díaz-Comeche A., Oliver S., Juste B., et al. Monte Carlo study of neutron spectra unfolding for a proton beam using MLEM // Radiation Physics and Chemistry. 2025. Vol. 233. P. 112702.
31. Radiationsafety/bssunfold: Python package for neutron spectrum unfolding from measurements obtained with Bonner Sphere Spectrometer (BSS) URL: https://github.com/Radiationsafety/bssunfold (дата обращения : 04.05.2026).
32. Radiation Safety Standards (NRB-99/2009) Sanitary Rules and Regulations. SanPin 2.6.1.2523-09. Moscow Publ., 2009. (in Russian).
33. Petoussi-Henss N., et al. Conversion coefficients for radiological protection quantities for external radiation exposures // Annals of the ICRP. 2010. Vol. 40, no. 2-5. P. 1–257.
34. Koslowsky M. Spectral Unfolding: A Mathematical Perspective // IAEA TECDOC SERIES. 2020. P. 97.
35. Thielmann A.F., Kumar M., Weisser C., et al. Mambular: A Sequential Model for Tabular Deep Learning // arXiv preprint arXiv:2408.06291. 2024.
36. Zhu C., Byrd R.H., Lu P., Nocedal J. Algorithm 778: L-BFGS-B: Fortran subroutines for large-scale bound-constrained optimization // ACM Transactions on mathematical software (TOMS). 1997. Vol. 23, no. 4. P. 550–560.
37. Chizhov A., Chizhov K. Dose assessment of personnel neutron irradiation on high-energy accelerators using a multi-sphere Bonner spectrometer // Mathematical Modeling. 2023. Vol. 7, no. 2. P. 63–64.
38. Chizhov A., Chizhov K. Optimization approach to neutron spectra unfolding with Bonner multi-sphere spectrometer // Mathematical Modeling. 2024. Vol. 8, no. 3. P. 89–90.
39. Tikhonov A.N., Goncharsky A.V., Stepanov V.V., Yagola A.G. Numerical methods for solving ill-posed problems. M.: Nauka (in Russian), 1990.
40. Aleinikov V.E., Bamblevskij V.P., Komochkov M.M., et al. Reference neutron fields for metrology of radiation monitoring // Radiation Protection Dosimetry. 1994. Vol. 54, no. 1. P. 57–59.
41. Awschalom M., Sanna R.S. Applications of Bonner sphere detectors in neutron field dosimetry. Fermi National Accelerator Lab., 1983.
42. Chizhov K., Chizhov A. Optimization of the Neutron Spectrum Unfolding Algorithm Using Shifted Legendre Polynomials Based on Weighted Tikhonov Regularization // Physics of Particles and Nuclei. 2025. Vol. 56, no. 6. P. 1395–1399. DOI: 10.1134/S106377962570056X.
43. Chizhov K., Bragin Yu., Sneve M.K., et al. The development and application of a method for assessing radionuclide surface contamination density based on measurements of ambient dose equivalent rate // Journal of Radiological Protection. 2019. Vol. 39, no. 2. P. 354.
44. Chizhov K., Bragin Yu., Sneve M.K., et al. Further development and application of a method for assessing radionuclide surface activity distribution and source location based on measurements of ambient dose equivalent rate. Examples for Andreeva Bay, Chernobyl NPP and Istiklol // Journal

of Radiological Protection. 2023. Vol. 43, no. 4. P. 041506. DOI: 10.1088/1361-6498/ad005c.

45. Chizhov K., Bragin Yu., Sneve M.K., et al. Further development and application of a method for assessing radionuclide surface activity distribution and source location based on measurements of ambient dose equivalent rate // Journal of Radiological Protection. 2023. Vol. 43, no. 4. P. 041505. DOI: 10.1088/1361-6498/ad005b.
46. Wang J., Zhou Y., Guo Z., Liu H. Neutron spectrum unfolding using three artificial intelligence optimization methods // Applied Radiation and Isotopes. 2019. Vol. 147. P. 136–143.
47. Jablonský J., et al. Benchmarks for current linear and mixed integer optimization solvers // Acta Universitatis Agriculturae et Silviculturae Mendelianae Brunensis. 2015. Vol. 63, no. 6. P. 1923–1928.